



## SILICATE GLASS COATINGS ON Ti-BASED IMPLANTS

A. PAZO<sup>1,2</sup>, E. SAIZ<sup>1</sup> and A. P. TOMSIA<sup>1</sup>

<sup>1</sup>Lawrence Berkeley National Laboratory, Berkeley, CA, U.S.A. and <sup>2</sup>Instituto de Ceramica, Universidad de Santiago, Santiago, Spain

**Abstract**—Coating Ti-based implants with bioactive materials, able to form hydroxyapatite layers *in vivo*, facilitates joining between the prostheses and bone and increases the long-term stability of the implants. The present work describes a new route to coat Ti alloys with bioactive silica-based glasses. A new family of potentially bioactive glasses that display good physical compatibility with Ti has been developed. In order to fabricate dense coatings, glass powder has been painted over the metal substrates and the assemblies have been fired to make the glass flow and adhere to the metal. The reactions that occur between the glass and the metal during this process have been studied by thin film X-ray diffraction and electron microprobe. By tailoring the glass composition and controlling the firing conditions (atmosphere, temperature and time) homogeneous coatings with good adhesion to the metal have been prepared. The physical characteristics of the glasses and their behavior in simulated body fluid are also reported. © 1998 Acta Metallurgica Inc.

### 1. INTRODUCTION

Due to their biocompatibility and mechanical properties, Ti and Ti-based alloys are widely used in the fabrication of prosthetic implants. The lives of Ti-based prostheses are, in many cases, limited by their inadequate adhesion to bone. In order to improve adhesion, the implants are often coated with a layer of hydroxyapatite (HA). Synthetic HA,  $\text{Ca}_{10}(\text{PO}_4)_6(\text{OH})_2$ , is bioactive [1,2] and similar in structure and composition to the mineral component of vertebrae hard tissue. High-resolution microscopy studies have shown that it can attach epitaxially to bone [3].

The most commonly used techniques to fabricate HA coatings are plasma spraying and ion sputtering. Plasma spraying produces porous coatings with thickness ranging from 50 to 200  $\mu\text{m}$ . However, HA changes in chemical composition and structure during the plasma processes [4–7] and the final layer does not adhere well to the metal [8]. Ion sputtering produces very thin (1  $\mu\text{m}$ ) and dense HA layers in which the lack of open porosity hinders the desired osseointegration. Both techniques are “line of sight” methods, and thus, they are not suitable for coating complicated shapes.

The objective of this work is to develop a method to produce bioactive (able to form HA layers *in vivo* [9]) coatings on Ti-based materials in order to improve their adhesion to bone. A simple enameling technique is used to coat Ti and Ti-based alloys with bioactive or biocompatible glasses. This method is useful for glazing complicated shapes with layers of controlled thickness. The glasses can be used alone or mixed with HA. The main tasks are to develop bioactive glasses that have good physical compatibility with Ti and to design a firing schedule in which detrimental reactions are con-

trolled. The final result should be a bioactive coating that presents good adhesion to the metal.

### 2. EXPERIMENTAL

Three glasses from the  $\text{SiO}_2\text{--Na}_2\text{O--K}_2\text{O--CaO--MgO--P}_2\text{O}_5$  system were prepared starting from silica powder (99.9%) and reagent grade  $\text{CaCO}_3$ ,  $\text{NaPO}_3$ ,  $\text{Na}_2\text{CO}_3$ ,  $\text{K}_2\text{CO}_3$  and MgO. The compositions, presented in Table 1, were derived from Bioglass<sup>®</sup> (originally developed by Hench [9]) by increasing the  $\text{SiO}_2$  content and partially substituting  $\text{K}_2\text{O}$  for  $\text{Na}_2\text{O}$  and MgO for CaO. The objective was to reduce the coefficient of thermal expansion ( $\alpha$ ) of Bioglass ( $14 \times 10^{-6}/^\circ\text{C}$ ) [10] and make it compatible with that of Ti ( $9.4 \times 10^{-6}/^\circ\text{C}$ , at  $400^\circ\text{C}$ ). In order to assess the effects of titania dissolution on bonding and bioactivity, a small quantity of  $\text{TiO}_2$  was added in composition A-6. For comparative purposes, Bioglass<sup>®</sup> was also prepared and included in the *in vitro* and coating experiments.

The glasses were synthesized by mixing the ingredients in isopropyl alcohol using a high-speed stirrer. After drying ( $110^\circ\text{C}$ , 48 h), the powder mixture was fired in a Pt crucible for 4 h at  $1400^\circ\text{C}$ . The melt was cast into a graphite mold to obtain large pieces for property evaluation or quenched in a water bath to fracture into small pieces. Thermal and mechanical properties of the glasses were measured by dilatometry and indentation techniques, respectively.

Behavior of the glasses in body fluid was studied by *in vitro* tests. Glass plates ( $10 \times 10 \times 1$  mm) and powders (average particle size  $\sim 10 \mu\text{m}$ ) were soaked in simulated body fluid (SBF) [11] at a constant temperature of  $36.5^\circ\text{C}$  for times varying up to

Table 1. Glass compositions (in wt%)

Designation	SiO <sub>2</sub>	Na <sub>2</sub> O	K <sub>2</sub> O	CaO	MgO	P <sub>2</sub> O <sub>5</sub>	TiO <sub>2</sub>
Bioglass <sup>®</sup>	45.0	24.5		24.5		6.0	
A-3	54.5	12.0	4.0	15.0	8.5	6.0	
A-5	56.5	11.0	3.0	15.0	8.5	6.0	
A-6	54.8	10.7	2.9	14.6	8.2	5.8	3.0

50 days. For all samples, the pH was monitored as a function of time. For the powder specimens, the pH at the glass-SBF interface was measured using two identical ion sensitive field effect transistors (ISFET). The pair of ISFETs were arranged in a differential measurement set-up described elsewhere [12, 13]. The ISFET sensitive membrane consisted of a 100  $\mu\text{m}$  thick layer of Si<sub>3</sub>N<sub>4</sub> over a 78 nm thick layer of SiO<sub>2</sub>. The sensitive area of each chemical sensor is 400  $\times$  200  $\mu\text{m}^2$  and the size of the whole chip was 2.4  $\times$  1.35 mm.

After soaking, the plates were analyzed by thin film X-ray diffraction (TF-XRD) and scanning electron microscopy (SEM). Elemental analysis was performed both by energy dispersive (EDS) and wavelength dispersive (WDS) methods.

To produce the glass coatings, glass powder with particle size < 50  $\mu\text{m}$  was first obtained by milling in a planetary mill with agate balls. A suspension of the powder in isopropanol was then deposited over Ti and Ti-6Al-4V plates (99.0% purity, 10  $\times$  10  $\times$  1 mm), which had been previously polished with 1  $\mu\text{m}$  diamond and cleaned in acetone and ethanol. The samples were then fired in a Unitek dental furnace by preheating to 600°C in air followed by simultaneously evacuating the oven to 1.3  $\times$  10<sup>5</sup> Pa and heating (heating rate, 40°C/min) to the desired temperature (between 700 to 1000°C). Once the temperature was reached, the vacuum was released by the furnace. The final coating thickness ranged between 25 and 150  $\mu\text{m}$ .

Polished cross-sections were examined by reflected light optical microscopy and SEM with associated EDS and WDS. Interfacial reactions and diffusion were studied by electron microprobe analyses (EPMA) of the cross-sections. Reactivity was also studied by TF-XRD. Thin, Ti foils (0.08 mm) were coated, fired, and then bent in order to remove the glass layer. TF-XRD was performed on both the substrate and glass sides of the interface. The samples were also analyzed by SEM-EDS.

In order to reveal the relative crack resistance and weak fracture path, the adherence of the coatings was qualitatively evaluated by indentation. Vickers indentation at the glass/metal interface was

performed on polished cross-sections using 0.5–2.2 kg loads in ambient air.

### 3. RESULTS AND DISCUSSION

#### 3.1. Glass properties

The bulk properties of the glasses are presented in Table 2. As expected, increases in SiO<sub>2</sub> and MgO content of the glasses decrease the thermal expansion coefficients and increase the softening points.

Figure 1 shows pH evolution of SBF during the *in vitro* tests. For all glasses, a rapid increase in pH at the glass-liquid interface is observed. The pH of the interface reaches values  $\geq 9$  in less than 1 min. Evolution of the pH in the solution is slower, remaining < 9 for times up to 7 days.

During soaking in SBF, a HA layer forms on the surface of the TiO<sub>2</sub> free glasses (Fig. 2). It is observed that HA forms faster on the Bioglass<sup>®</sup> surface than on the new compositions. *In vivo* tests have also shown that the A-3 glass is bioactive [14]. Kokubo [15] reported that the compositional and structural characteristics of the HA formed on the surface of a bioactive glass are common to those of human bone HA. It is thus expected that a strong bond will form between the newly formed HA and bone.

Glasses with lower SiO<sub>2</sub> content have a more open network structure, which enables a faster proton-alkali exchange and a higher pH increase. According to the solubility diagram for Ca phosphate minerals proposed by Limsay and Ulek [16], pH values greater than 9 are required for HA precipitation. The HPO<sup>2-</sup> concentration in SBF is 10<sup>-3</sup> M, and consequently, the mechanism of HA formation on the surfaces of the A-3 and A-5 glasses seems to be that proposed by Aza *et al.* [13]. That is, an increase of pH at the glass-SBF interface occurs due to ionic exchange of H<sub>3</sub>O<sup>+</sup> from the SBF for soluble cations in the glass such as Na<sup>+</sup>, K<sup>+</sup>, Ca<sup>2+</sup>, etc. This exchange leaves a silica-rich hydrogel layer on the glass prior to the formation of HA. At this high pH, part of the silica hydrogel is dissolved in the SBF and, subsequently, HA precipitates on the surface.

Table 2. Glass properties

Designation	Softening point (°C)	CTE (10 <sup>-6</sup> /°C)	Vickers hardness <i>H<sub>v</sub></i> (GPa)
Bioglass <sup>®18</sup>	555	14	–
A-3	575	11.6	3.5–4.0
A-5	637	8.5	3.2–3.9
A-6	615	–	–



Fig. 1. SEM micrograph of the HA crystals formed on the surface of an A-5 glass plate after soaking 50 days in SBF.

However, despite a pH evolution similar to that of glass A-5, the TiO<sub>2</sub>-containing glass (A-6) does not form HA even after soaking for 50 days. This agrees with the results reported by Gross and Strunz [17, 18] about the effect of polyvalent cations

dissolution on bioactivity. EDS analysis reveals a high Ti concentration on the A-6 glass surface after the test. Hench attributed the destructive effect of polyvalent cations on bone bonding to the precipitation of these cations as oxides, hydroxides or carbonates [19]. This could be the reason for the large Ti concentration detected on the surface of the A-6 glass. Nevertheless, even if not directly bioactive, this glass is still a candidate for composite or layered HA-glass coatings.

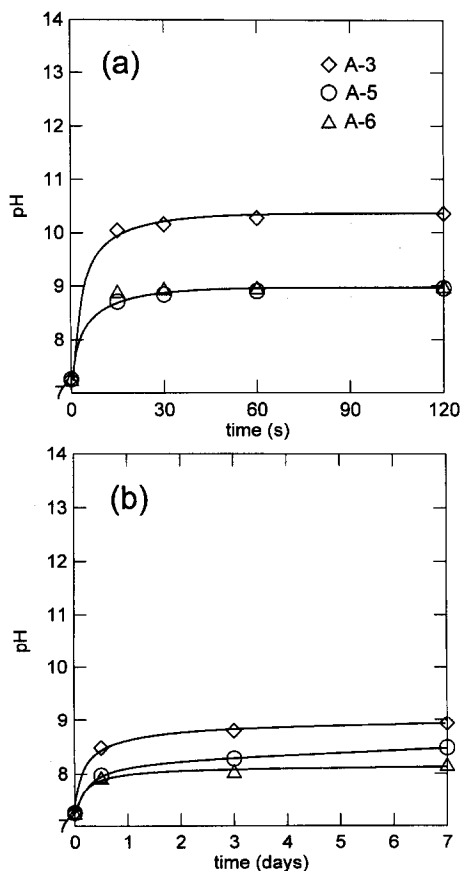


Fig. 2. pH evolution of SBF after immersion of 3 g of glass powder in 20 ml of fluid. The pH was measured at the glass-SBF interface (a) and in the liquid far away from the interface (b).

### 3.2. Coating fabrication

Firing temperature and time greatly affect the stability of the coatings prepared using the new glasses. At temperatures < 750°C, porous layers form with poor adhesion to the metal. Temperatures higher than 850°C and times longer than 1 min result in dewetting and/or reaction with the formation of bubbles. Excellent adhesion is only obtained after firings at 800 ≤ T < 850°C for periods of time < 1 min (Fig. 3). In this case, a qualitative assessment of the interfacial strength by indentation shows no interfacial fracture; cracks do not propagate along the interface but instead tend to be driven into the glass (Fig. 4). The addition of small amounts of TiO<sub>2</sub> (A-6 glass) slightly broadens the time-temperature range appropriate to achieve a good bond (Fig. 5). Experiments performed at heating rates slower than 40°C/min resulted in excessive oxidation of the metal before the glass melts. No significant differences in adhesion are found between Ti and Ti-6Al-4V substrates. Experiments performed with Bioglass<sup>®</sup> are unsuccessful due to the fast crystallization rate of the glass that leads to very porous coatings, which are not bonded to the metal (Fig. 6).

Electron microprobe analysis of the samples with optimum adhesion did not show any appreciable change in the composition of the glasses after firing.

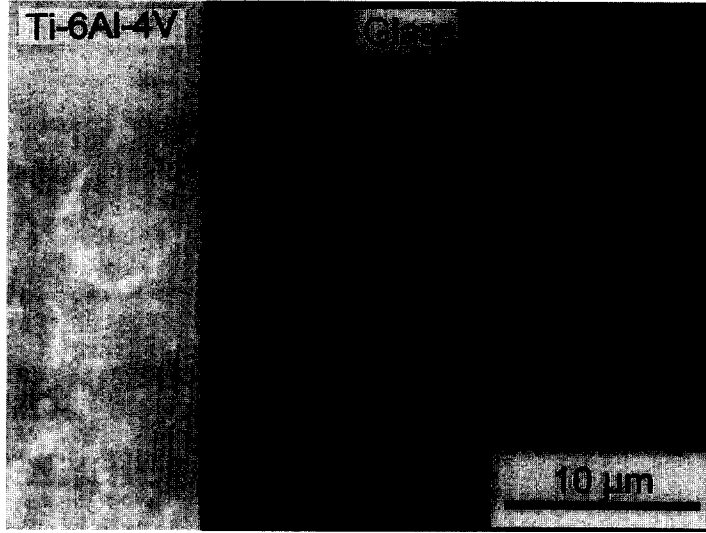


Fig. 3. Cross-section of an A-6 coating on Ti-6Al-4V fired 1 min at 850°C.

In these cases EPMA did not detect any reaction products at the interface (Fig. 7). TF-XRD of the interface showed the presence of a  $TiO_x$  layer on substrates fired at temperatures below the glass softening point. It also detects a  $Ti_5Si_3$  layer attached to the metal (Fig. 8) in coatings fired at  $T \geq 850^\circ C$  for times bigger than 1 min.

Figure 9 shows a SEM image of the substrate surface after removing an A-6 coating fired at 850°C for 1 min. Small pieces of glass still bonded

to the metal are observed. EDS analysis on the surface shows only the Ti and Si peaks corresponding to the titanium silicide detected by XRD. The silicide layer must be very thin since it is not detected by EPMA on the cross-section. Some areas where the silicide has been removed with the glass are observed; EDS analysis of these areas detects only Ti.

Several reactions occur during firing. First, while heating, gas easily diffuses through the porous deposited layer and a thin oxide skin forms on the surface of the metal. At temperatures higher than the softening point, the glass layer sinters and flows. The inner glass/metal interface becomes sealed from the external atmosphere, and the glass dissolves the  $TiO_x$  layer and starts to react with the substrate. The formation of silicides observed by TF-XRD occurs according to the reaction:

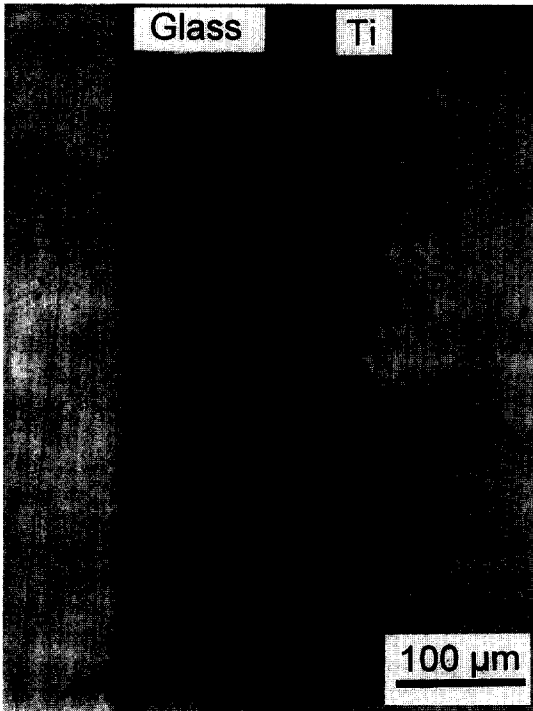


Fig. 4. Optical micrograph of a cross-section of A-6 coating on Ti (fired 1 min at 850°C) after interfacial indentation (2.2 kg load, 15 s). The indentation cracks run away from the interface into the glass.

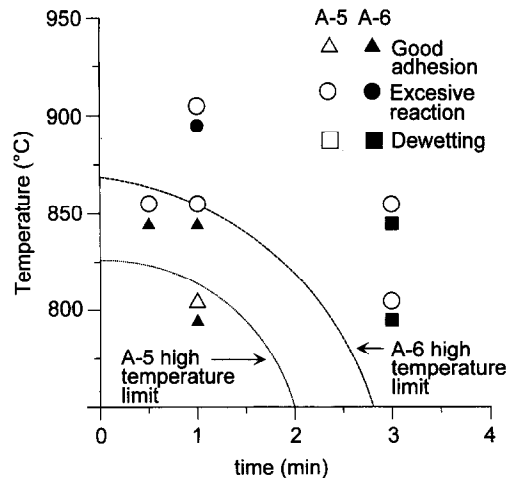


Fig. 5. Effect of firing temperature and time on coating quality for glasses A-5 and A-6.

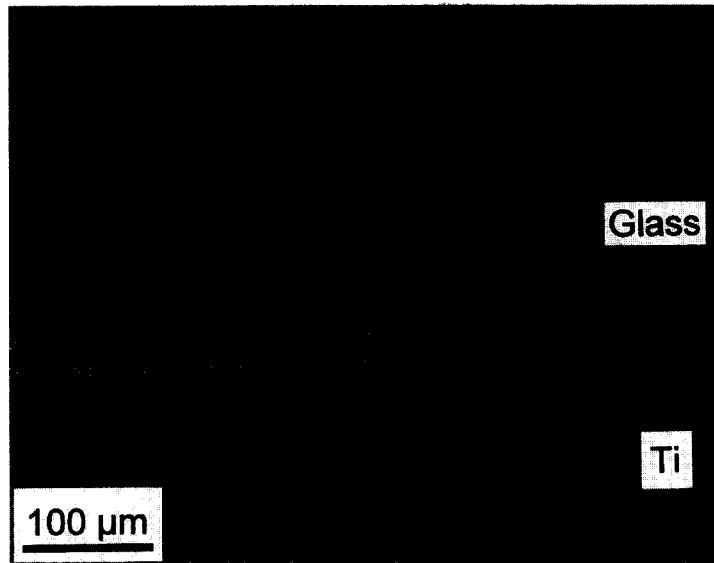
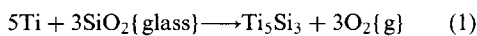


Fig. 6. Optical micrograph of a cross-section of a Bioglass<sup>®</sup> coating on Ti fired at 900°C for 1 min. Extensive porosity and lack of adhesion are visible.



Concurrently, at the periphery of the coating, the equilibrium reaction at the furnace  $P(\text{O}_2)$  takes place and the metal oxidizes to form  $\text{TiO}_2$ . In a previous paper the presence of an oxide layer at the coating periphery growing inward through the triple junction into the glass/metal interface has been shown. The finite angle of the glass over this layer is responsible for the dewetting observed at longer firing times.

Excessive reaction and formation of silicides is undesirable; silicides are usually brittle, have higher thermal expansion than Ti ( $\alpha_{\text{Ti}_5\text{Si}_3} = 11 \times 10^{-6}/^\circ\text{C}$ ), and result in bubble formation due to the liberation of oxygen gas during the reaction. On the other hand, the formation of a thick oxide layer at the interface results in weak bonding due to the porosity of the oxide and its physical incompatibility with the metal.

The best coatings fabricated with the new glasses have been impossible to remove from the metal. Even after repeated bending of the substrate, a thin glass layer remains attached to the metal. In these cases, our analytical techniques have failed to clearly identify any interfacial products.

Due to the glass dissolution to form HA, a minimum coating thickness is required to preserve its stability in body fluids. Coatings with thickness up to 150  $\mu\text{m}$  without crazing have been prepared using A-5 and A-6 glasses. However, Fig. 10 shows cracking after cooling a 100  $\mu\text{m}$  A-3 glass coating on Ti-6Al-4V. The cracks are due to the thermal stresses resulting from the thermal expansion difference between the glass and metal. Cracks do not appear in thinner coatings ( $\sim 25 \mu\text{m}$ ). The maximum possible thickness without cracking is given by the

thermal expansion mismatch. For example, for similar geometries and firing temperatures, the relation between thermal stresses in the A-3 and A-5 glasses is:

$$\frac{\alpha_{\text{A-3}}}{\alpha_{\text{A-5}}} \approx \frac{\alpha_{\text{A-3}} - \alpha_{\text{Ti}}}{\alpha_{\text{A-5}} - \alpha_{\text{Ti}}} > 4 \quad (2)$$

Consequently, it is possible to fabricate thicker glazes without cracking using the A-5 glass. In general,  $\text{SiO}_2$ -rich glasses show lower bioactivity, but their lower  $\alpha$  (closer to Ti) allows the fabrication of thicker coatings.

In summary, the appropriate range of firing temperatures is delimited by the glass softening and viscosity on one side and by the glass/metal reactivity on the other. To achieve a good bond, it is necessary to control reactivity such that only very thin interfacial layers are present at the end of the process, thus avoiding formation of bubbles or thick, brittle layers. Our tests have shown that control of the furnace atmosphere is critical in the process; previous experiments performed in argon resulted in uncontrolled reactivity and no adhesion [21]. The addition of small amounts of titania to the glass (A-6 glass) reduces the dissolution rate of the oxide formed during heating, makes the reactivity more controllable, and broadens the time-temperature range appropriate to achieve a good bond. When using HA-glass mixtures, reactivity between the glass and HA is another factor to consider; in this regard, the limited reactivity between the A-3 glass and HA has been previously reported [20].

The optimum glass composition must be formulated such that bioactive coatings with the required thickness can be prepared. Using the glasses developed in this work, it has been possible to fabricate coatings up to 150  $\mu\text{m}$  thick with potentially bioac-

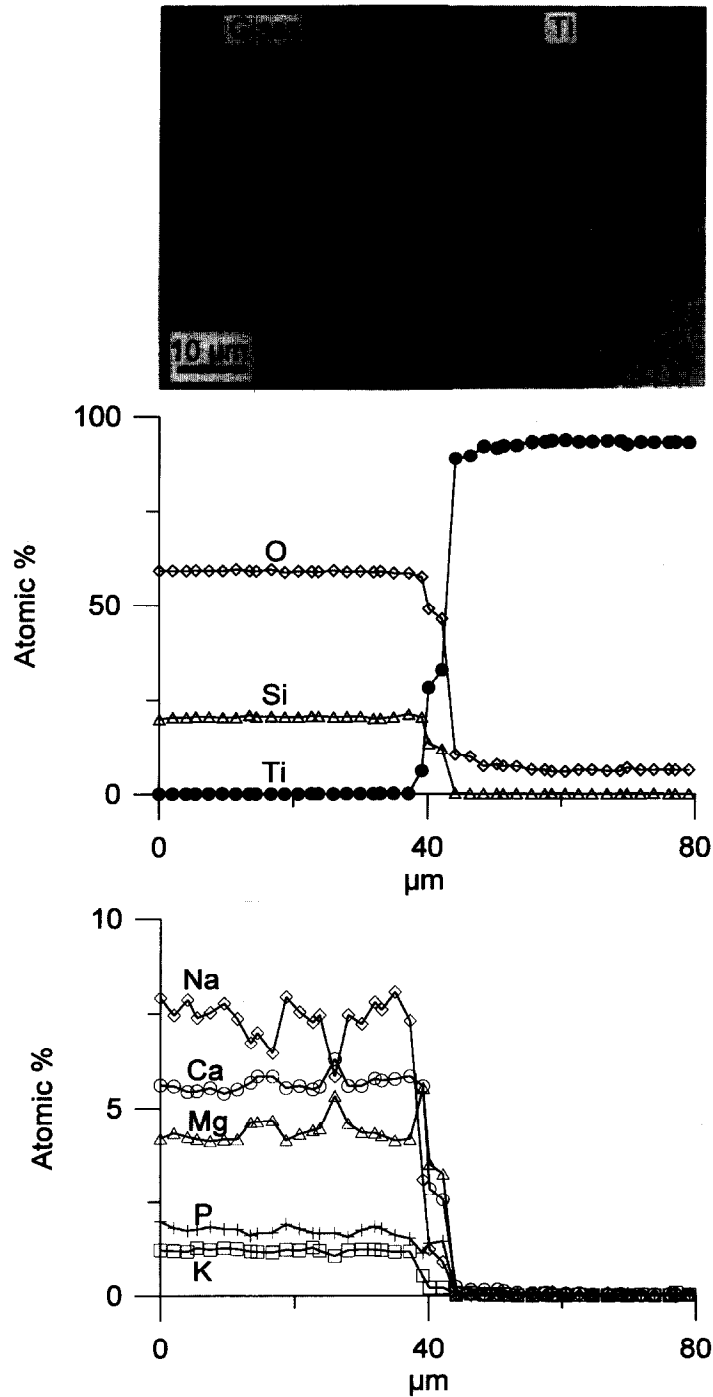


Fig. 7. SEM and associated EPMA of a cross-section of A-5 coating on Ti (fired 1 min/800°C). No interdiffusion or interfacial products can be detected.

tive compositions (glass A-5). The *in vitro* behavior of glass coatings on Ti and Ti alloys will presumably be the same as that with the bulk glasses since no change in composition is detected after the coating procedure. By contrast, attempts to fabricate useful coatings using the original Bioglass® have been marred by poor densification and adhesion

resulting from the high thermal stresses due to its thermal expansion coefficient mismatch with Ti.

#### 4. CONCLUSIONS

In order to fabricate bioactive coatings on Ti-based implants a new family of potentially bioactive glasses belonging to the  $\text{SiO}_2\text{-Na}_2\text{O-K}_2\text{O-CaO-}$

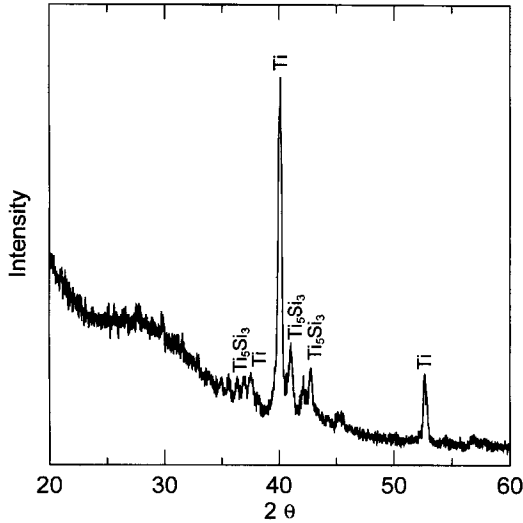


Fig. 8. TF-XRD of the substrate surface after removal of an A-5 coating fired 1 min at 850°C. XRD detects the presence of a thin  $\text{Ti}_3\text{Si}_5$  layer.

$\text{MgO-P}_2\text{O}_5$  system has been developed. It has been found that some glasses in the system present excellent bioactivity and that by controlling the processing conditions (firing time, temperature and atmosphere) it is possible to fabricate coatings that show good adherence to Ti and Ti alloys. However, due to their low  $\text{SiO}_2$  content, these glasses have a higher thermal expansion coefficient than is desirable. This often results in cracking during the fabrication of thick coatings. Thin coatings neither crack nor delaminate and these compositions may actually be useful as such. By tailoring the composition, it is possible to prepare glasses with lower  $\alpha$  that are equally adherent, potentially bioactive and can be used to fabricate coatings as thick as 150  $\mu\text{m}$ .

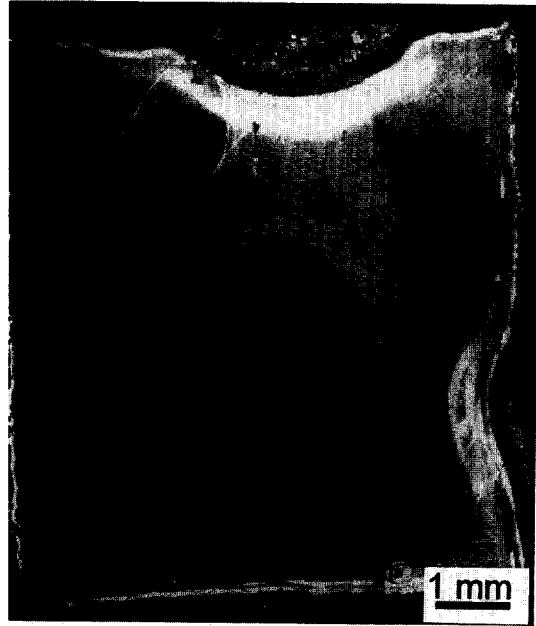


Fig. 10. Stereographic micrograph of a 100  $\mu\text{m}$  thick A-3 glass coating on Ti-6Al-4V (fired 3 min at 800°C). Extensive cracking due to thermal stresses is observed.

The presence of a small amount of  $\text{TiO}_2$  in the glass yields a broader firing range and reduced reactivity. Despite the fact that this glass is not directly bioactive, it can be useful for composite or layered glass/HA coatings.

*Acknowledgements*—This work was supported by the NIH/NIDR grant 1R01DE11289. A.P. wishes to thank the Ministry of Education and Science of Spain for the postdoctoral fellowship given to her in the National Program of Fellowships for Formation of Researchers in Foreign Countries.

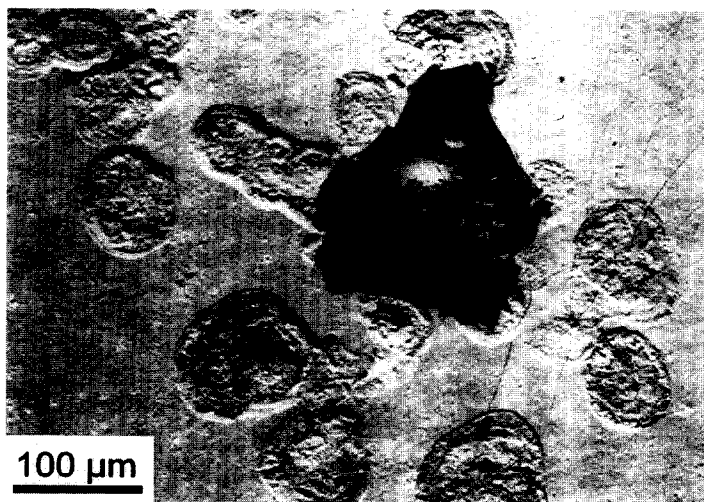


Fig. 9. SEM image of the metal surface after removing an A-6 coating fired 1 min at 850°C. Bits of glass are still present on the metal. The footprints correspond to areas where the interfacial silicide layer was removed with the glass.

## REFERENCES

1. Donath, K., Reaction of tissue to calcium phosphate ceramics, in *Osseo-Integrated Implants*, Vol. 1, ed. G. Heimke. CRC Press, Boca Raton, FL, 1990, pp. 99–125.
2. Kay, J. F., *Dent. Clin. North. Am.*, 1992, **36**, 11–18.
3. Bonfield, W. and Luklinska, Z. B., High-resolution electronic microscopy of a bone implant interface, in *The Bone-Biomaterial Interface*, ed. J. E. Davies. University of Toronto Press, 1991, pp. 89–94.
4. Lacefield, W. R., Rigney, E. D., Lucas, L. C., Ong, J. and Gantenberg, J. B., in *Sputter Deposition of Ca-P Coatings Onto Metallic Implants*, ed. P. Vincenzini. Elsevier, 1991.
5. de Groot, K., *The Cent. Mem. Is. Ceram. Soc. Jpn.*, 1991, **99**, 943.
6. Koch, B., Wolke, J. G. C. and de Groot, K., *J. Biomed. Mater. Res.*, 1990, **24**, 655.
7. Hastings, G. W., Dailly, D. and Morey, S., in *Bioceramics*, Vol. 1, ed. H. Ohnishi, H. Aoki and K. Sawai. Ishyaku EuroAmerica, 1989, pp. 355–358.
8. Cook, S. D., Thomas, K. A., Dalton, J. E., Volkman, T. K., Whitecloud, T. S. III and Kay, J. F., *J. Biomed. Mater. Res.*, 1993, **27**, 1501–1507.
9. Hench, L. L., Bioactive ceramics, in *Bioceramics: Material Characteristics vs In Vivo Behaviour*, Annals of the New York Academy of Sciences, Vol. 523, ed. P. Ducheyne and J. E. Lemmons. New York, NY, 1988.
10. Krajewski, A., Ravaglioli, A., De Portu, G. and Visani, R., *Am. Ceram. Soc. Bull.*, 1985, **64**, 679.
11. Gamble, J., *Chemical Anatomy, Physiology and Pathology of Extracellular Fluid*. Harvard University Press, Cambridge, 1967.
12. Merlos, A., Garcia, I., Cane, C., Esteve, J., Bartroli, J. and Jimenez, C., in *Proceedings of the 5th Conference on Sensors and Their Applications*. Edinburgh, September 1991, p. 127.
13. de Aza, P. N., Guitian, F., Merlos, A., Lora-Tamayo, E. and de Aza, S., *J. Mater. Sci. Mater. Medicine*, 1996, **7**, 399.
14. Pazo, A., Ceramic Biomaterials II: Obtaining and Properties of Bioceramic Coatings on Titanium. Ph.D. in microcard of Universidad de Santiago de Compostella, No. 481. Ed. Servicio de Publicaciones e Intercambio Científico de la Universidad de Santiago de Compostella, ETD S.A., Barcelona, Spain, 1995.
15. Kokubo, T., Bonding mechanism of bioactive glass-ceramic A-W to living bone, in: *Handbook of Bioactive Ceramics*, Vol. 1, Bioactive Glasses and Glass Ceramics, ed. T. Yamamuro, L. L. Hench and J. Wilson. CRC Press, Boca Raton, FL, 1990.
16. Limsay, W. L. and Ulek, P. L., in *Minerals in Soil Environments*. Soil Science Society of America, Madison, WI, 1977.
17. Gross, U. and Strunz, V., *J. Med. Mater. Res.*, 1980, **14**, 607.
18. Gross, U. and Strunz, V., in *Clinical Applications of Biomaterials*, ed. A. J. C. Lee, T. Albrektsson and P. Branemark. John Wiley and Sons, New York, NY, 1982.
19. Hench, L. L., Bioactive glasses and glass-ceramics: A perspective, in *Handbook of Bioactive Ceramics*, Vol. 1, ed. T. Yamamuro, L. L. Hench and J. Wilson. CRC Press, Boca Raton, FL, 1990, pp. 7–23.
20. Pazo, A., Santos, C., Guitian, F., Tomsia, A. P. and Moya, J. S., *Scripta Metall.*, 1996, **34**, 1729.
21. Pazo, A., Saiz, E. and Tomsia, A. P., Bioactive coatings on Ti and Ti-6Al-4V alloys for medical applications, in *Ceramic Microstructures '96*. Plenum Press, New York, in press.